Development of a Potassium-Ion-Responsive Star Copolymer with Controlled Aggregation/Dispersion Transition

Noriko Nakamura, Seiichi Ohta, Mariko Yamada, Yukimitsu Suzuki, Natsuko F. Inagaki, Takeo Yamaguchi, and Taichi Ito*

Read Online

ACCESS | Metrics & More | Article Recommendations | Supporting Information

ABSTRACT: Stimuli-responsive star polymers are promising functional materials whose aggregation, adhesion, and interaction with cells can be altered by applying suitable stimuli. Among several stimuli assessed, the potassium ion (K^+), which is known to be captured by crown ethers, is of considerable interest because of the role it plays in the body. In this study, a K^+-responsive star copolymer was developed using a polyglycerol (PG) core and grafted copolymer arms consisting of a thermo-responsive poly(N-isopropylacrylamide) unit, a metal ion-recognizing benzo-18-crown-6-acrylamide unit, and a photoluminescent fluorescein O-methacrylate unit. Via optimization of grafting density and copolymerization ratio of grafted arms, along with the use of hydrophilic hyperbranched core, microsized aggregates with a diameter of 5.5 μm were successfully formed in the absence of K^+ ions without inducing severe sedimentation (the lower critical solution temperature (LCST) was 35.6 °C). In the presence of K^+ ions, these aggregates dispersed due to the shift in LCST (47.2 °C at 160 mM K^+), which further induced the activation of fluorescence that was quenched in the aggregated state. Furthermore, macrophage targeting based on the micron-sized aggregation state and subsequent fluorescence activation of the developed star copolymers in response to an increase in intracellular K^+ concentration were performed as a potential K^+ probe or K^+-responsive drug delivery vehicle.
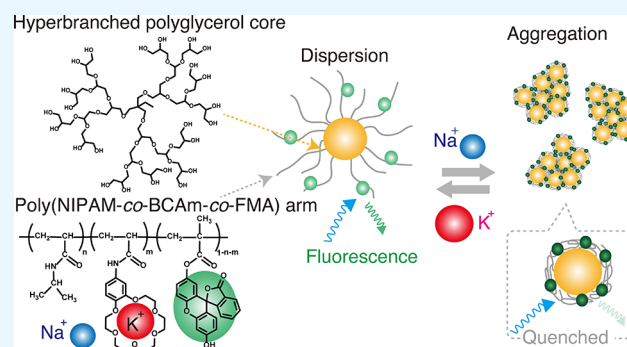

INTRODUCTION

Stimuli-responsive polymers can have their chemical and physical properties altered in response to internal and/or external stimuli.[1] Examples of such polymers include polymer films,[2,3] brushes,[4,5] hydrogels,[6,7] and colloidal particles,[8] which have been widely investigated for various applications. Stimuli-responsive star polymers[9,10] have received considerable attention because their arm structure, density, and diameter can be flexibly designed. In addition, several core structures have been reported, which make the design of star polymers highly fascinating. Additionally, star polymers behave as soft colloidal particles[11–13] owing to the charge, hydrophilicity/hydrophobicity, etc., afforded by the multiple termini of these polymers.[10] Thus, they have the potential for biomedical applications as drug delivery carriers,[14,15] hydrogels,[16–19] and imaging agents.[20,21] In the physiological environment, various stimuli (e.g., temperature,[19] pH,[20] redox,[14,15,17] metal ions,[16,18] and reactive oxygen species[21]) have been used to induce structural transition and the resultant functional switching of star polymers. In addition, the structural transition of each star polymer can induce secondary structural changes in the higher hierarchies, such as the formation and collapse of colloidal superstructures, including aggregation and dispersion.[22]

Ion-responsive star polymers are promising for applications in the biomedical field because many ions are ubiquitous and play important roles in our bodies. Potassium (K^+) and sodium ions (Na^+) are essential for maintaining the balance between intracellular and extracellular ion concentrations and for regulating osmotic pressure across cellular membranes. It is also known that the K^+ flux into phagosomes activates proteases to disrupt the bacteria in phagocytic cells.[23] Since K^+ ions play such an important role in our bodies, K^+-responsive[24–27] materials utilizing crown ether-functionalized molecules[24–27] have attracted research attention for decades. Among these, poly(N-isopropylacrylamide-co-benzo-18-crown-6-acrylamide) [poly(NIPAM-co-BCAm)][28] has been studied for various applications. Poly(N-isopropylacrylamide) (PNIPAM) is a thermo-sensitive polymer. The crown ether moiety of BCAm can form complexes with K^+, which alters its
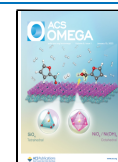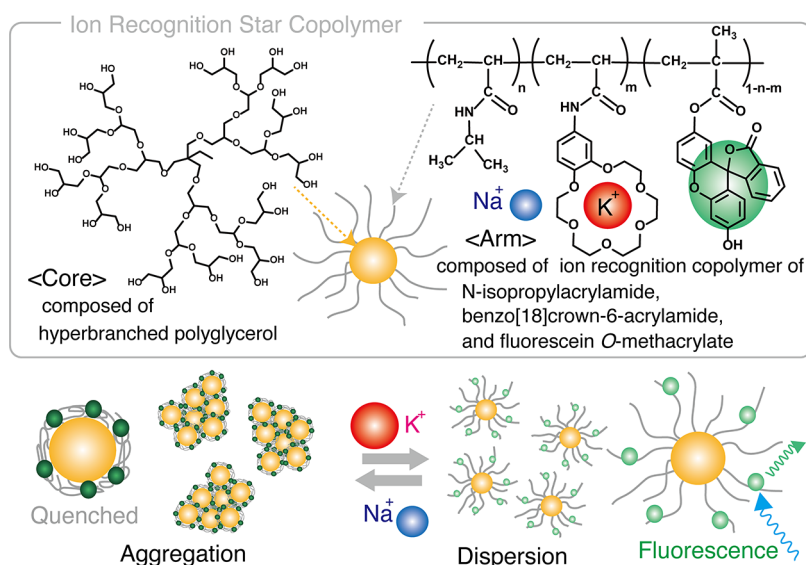
Figure 1. Schematic of the chemical structures of star copolymers and their K$^+$-responsive dispersion/aggregation transition and PL switching.

hydrophilicity and induces the phase transition of poly-(NIPAM-*co*-BCAm). Owing to their K$^+$-responsiveness, hydrogels,[29,30] membranes,[31−34] colloidal particles, and microspheres[35,36] have been widely investigated. Using poly-(NIPAM-*co*-BCAm) as the arms of star polymers, novel ion-responsive star polymers are expected to be developed. However, star copolymer utilizing poly(NIPAM-*co*-BCAm) as star arms has not been explored yet.

The presence of several termini for chemical modification makes hyperbranched polymers suitable for use in the core architecture of star polymers.[37,38] For example, hyperbranched polyglycerol (HPG), which has several hydroxyl groups at its termini, is expected to serve as a precursor of the core macroinitiator.[39,40] In addition, since HPG is composed of an ethylene oxide backbone similar to poly(ethylene glycol) (PEG), good biocompatibility and hydrophilicity can be expected. HPG has attracted considerable attention as an alternative to dendrimers and PEG biomaterials because of its relatively low cost, facile synthetic route,[41] and low immunogenicity.[42] However, HPG has not been explored as a core for K$^+$-responsive star polymers.

In this study, we developed a K$^+$-responsive star copolymer using an HPG-based macroinitiator core and grafted copolymer arms consisting of (1) a thermo-responsive NIPAM unit, (2) a metal ion-recognizing benzo-18-crown-6-acrylamide (BCAm) unit, and (3) a fluorescent fluorescein *O*-methacrylate (FMA) unit. The dispersion/aggregation transitions of the star copolymers in response to temperature and K$^+$ concentration, along with their resulting photoluminescence (PL) switching, were investigated (Figure 1). Furthermore, as an example of their potential biomedical applications, macrophage targeting of the developed star copolymers at the aggregation state was performed, followed by selective intracellular PL activation in response to the K$^+$ concentration increase in phagosomes.

MATERIALS AND METHODS

Materials. HPG (2890 g/mol) was purchased from Hyperpolymers GmbH (Freiburf, Germany). 2-bromoisobutyrylbromide, dehydrated pyridine, tetrahydrofuran (THF), hexane, formaldehyde, formic acid, tris(2-aminoethyl)amine

(TREN), sodium hydroxide (NaOH) dichloromethane, magnesium sulfate, chloroform, acetic acid, nitric acid, sodium carbonate, isopropyl alcohol, palladium-activated carbon (Pd 10%), dioxane, acryloyl chloride, toluene, copper(I) bromide, sodium chloride (NaCl), and potassium chloride (KCl) were purchased from FUJIFILM Waco Pure Chemicals Co. (Tokyo, Japan). Benzo[18]crown-6, *N*-isopropylacrylamide (NIPAM), and fluorescein *O*-methacrylate (FMA) were purchased from Sigma-Aldrich Co., LLC (St. Louis, MO). LysoTracker Red was purchased from Thermo Fisher Scientific Inc. (Waltham, MA).

Synthesis of HPG Macroinitiator. HPG was used as the core of a star copolymer, and the copolymer consisting of NIPAM, benzo[18]crown-6-acrylamide (BCAm), and FMA was attached as arms of the core. The terminal hydroxyl moieties of HPG were converted into 2-bromoisobytyryl groups using 2-bromoisobutyrylbromide to obtain the macroinitiator. The star arms were polymerized through atom transfer radical polymerization (ATRP) of NIPAM, BCAm, and FMA. First, HPG was dissolved in dehydrated pyridine, followed by nitrogen gas bubbling for 20 min, and then mixed with 2-bromoisobutylbromide (0.50, 0.75, and 1.00 equiv of hydroxyl groups of HPG) in an ice bath. After stirring overnight at room temperature, 2-bromoisobytyryl-terminated HPG (HPG-Br) was obtained as a macroinitiator after purification via filtration, washed with tetrahydrofuran (THF), reprecipitated in hexane, and dried under vacuum. 2-bromoisobytyryl group introduction on the HPG terminal ends was evaluated by proton nuclear magnetic resonance (^{1}H NMR) in CDCl$_3$. The introduction ratio was analyzed by the element assay.

Synthesis of Ligand for ATRP Polymerization. Next, tris[2-(dimethylamino)ethyl]amine (Me$_6$TREN) was synthesized as a ligand for ATRP polymerization according to previously reported procedures.[43] Formaldehyde (2.89 g) was mixed with formic acid (1.93 g) for 1 h on ice, and 0.448 g of TREN dissolved in 0.3 mL of water was added dropwise to the reaction solution. After stirring overnight at 95 °C, the reaction solution was cooled, and the pH was adjusted between 12 and 14 by adding saturated NaOH solution to obtain the oil phase. After purification by extraction with dichloromethane four

**Scheme 1. Synthetic Route to the Star Copolymer HPG-*g*-NIPAM-*co*-BCAm-*co*-FMA**
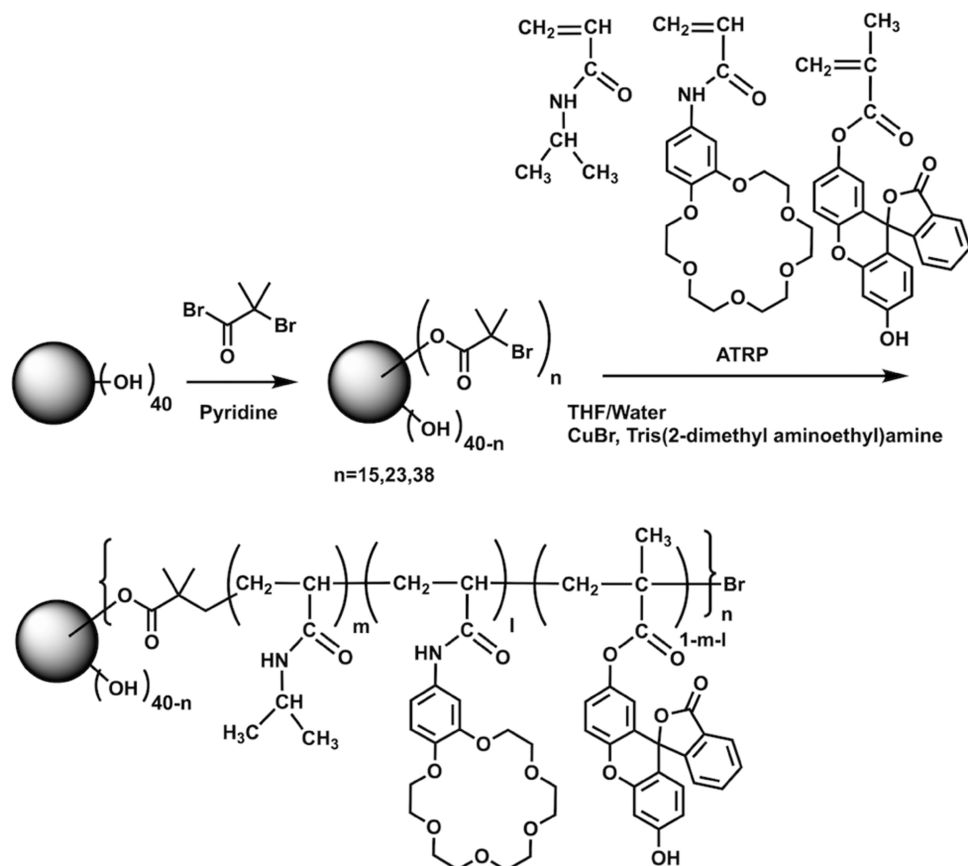
times, drying with magnesium sulfate, filtration, and evaporation, Me₆TREN was obtained as a yellow oil. Synthesis of Me₆TREN was confirmed through ¹H NMR measurement in CDCl₃.

ATRP Polymerization of HPG-*g*-NIPAM-*co*-BCAm-*co*-FMA. BCAm was synthesized from benzo[18]crown-6-ether according to the procedure described in our previous report.[32] Finally, ATRP of NIPAM, BCAm, and FMA was conducted using HPG-Br. HPG-Br (0.0076 g) was dissolved in 4 mL of THF, and then NIPAM (100 equiv of HPG-Br) was purified via recrystallization; BCAm (15 equiv of HPG-Br), FMA (1 equiv of HPG-Br), Me₆TREN (1 equiv of HPG-Br), and 1 mL of water were added to the reaction solution. After three freeze-thaw cycles, copper bromide (1 equiv of Br of HPG-Br) was added, followed by degassing. Subsequently, the polymerization reaction was conducted by stirring for 24 h at room temperature. The polymerization reaction was terminated by exposure to air. The resulting solution was purified by performing three dissolving–evaporating cycles into 10 mL of THF, dialysis against water for 3 days, and lyophilization. The resulting polymer was characterized using ¹H NMR and Fourier transform infrared (FT-IR) spectroscopy. The polymerization degree of each monomer of star arms was calculated from the conversion of each monomer, which is evaluated by ¹H NMR spectra of ATRP reaction solutions in DMSO-*d₆*. The NIPAM conversion of HPG-*g*-NIPAM was evaluated by comparing peaks from the isopropyl groups of monomers and polymers (3.4–4.1 ppm) with a peak from C═CH–C protons of residual NIPAM monomers (5.6 ppm). The polymerization degree of NIPAM and BCAm, which consisted of HPG-*g*-NIPAM-*co*-BCAm or HPG-*g*-NIPAM-*co*-BCAm-*co*-

FMA, was evaluated by comparing a peak from C═CH–C protons of residual NIPAM monomers (5.6 ppm) or a peak from C═CH–C protons of residual BCAm monomers (5.7 ppm) with the peaks from the isopropyl and crown ether groups of monomers and polymers (3.4–4.1 ppm). For this analysis, each peak area of isopropyl groups and crown ether groups was calculated from the signals at 3.4–4.1 ppm using the molar ratio of monomers added to the reaction mixture. We note that the signal from THF at 3.6 ppm also overlapped with the peaks at 3.4–4.1 ppm from isopropyl groups and crown ether groups. Since the peak area from THF at 3.6 ppm should be the same as the distinguishable peak of THF at 1.7 ppm, we subtracted the area of this peak from the peak areas at 3.4–4.1 ppm to eliminate the effect of THF.

Characterization of HPG-*g*-NIPAM-*co*-BCAm-*co*-FMA. The thermo- and potassium-ion-responsive phase transitions of the star copolymer were investigated by measuring the turbidity, morphology of aggregation, and hydrodynamic diameter. The turbidity of the obtained polymer in deionized water with 0, 5, 60, 80, 100, and 160 mM KCl was evaluated using a UV–vis spectrophotometer, V-630BIO (JASCO Co., Tokyo, Japan), at a wavelength of 420 nm. NaCl was added to the measurement solution to maintain a total ion concentration of 160 mM. The phase transition behavior was investigated in the range of 20–50 °C at an increasing rate of 1 °C/min. The morphology of the star copolymer in the aggregated state in the presence of 160 mM NaCl was observed by two-photon confocal laser scanning microscopy (LSM510 META NLO, Carl Zeiss Co. Ltd., Jena, Germany). The hydrodynamic diameter of the star copolymer in deionized water with 160 mM KCl or 160 mM NaCl was
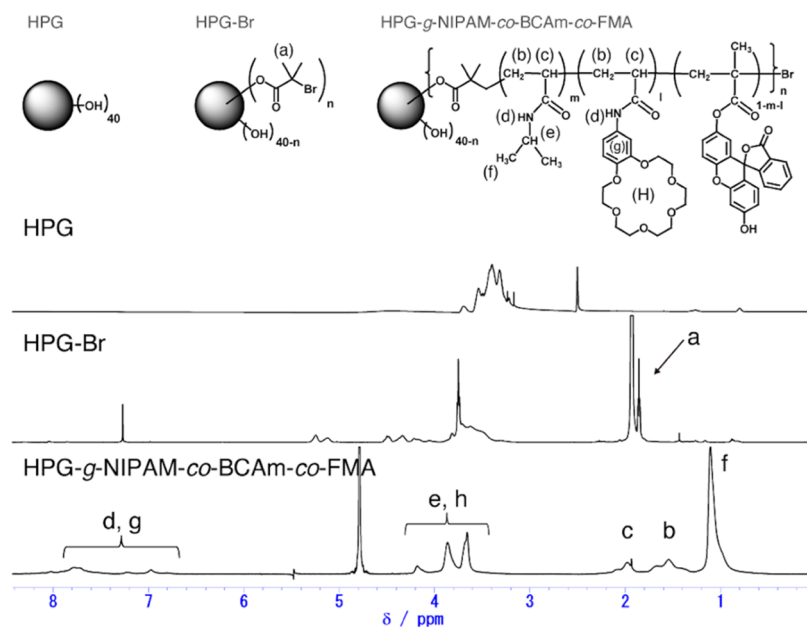
Figure 2. ^{1}H NMR spectra of HPG in DMSO-d_6, HPG-Br in CDCl$_3$, and HPG-g-NIPAM-co-BCAm-co-FMA in D$_2$O.

evaluated using a dynamic light scattering (DLS) LB-500 (HORIBA Ltd., Kyoto, Japan) with a diode laser (wavelength = 650 nm) at 20 and 40 °C.

Photoluminescence (PL) Switching Characterization of HPG-g-NIPAM-co-BCAm-co-FMA. Fluorescence spectra of the star copolymer in the presence of 160 mM KCl at 25, 30, 32.5, 35, 40, 45, and 50 °C were obtained using a fluorospectrometer FP-8200ST (JASCO Co., Tokyo, Japan) with an excitation wavelength of 468 nm and an emission wavelength of 480−600 nm. The fluorescence intensity at 521 nm was measured using 160 mM KCl or 160 mM NaCl at 25, 30, 35, 40, 45, and 50 °C.

Macrophage Uptake and PL Switching of HPG-g-NIPAM-co-BCAm-co-FMA. To investigate the interaction of HPG-g-NIPAM-co-BCAm-co-FMA aggregates with macrophages and K$^+$-responsive PL switching inside the cells, polymer aggregates were incubated with mouse macrophage cells. Mouse macrophage RAW 267.4 cells were maintained in RPMI medium with 10% fetal bovine serum and 1% penicillin−streptomycin at 37 °C and 5% CO$_2$. Cells were seeded on a 35 mm glass-bottom dish with a cell density of 5.0 × 10^3 cells/cm^2 and then incubated overnight. The cells were subsequently treated with a cell culture medium containing 1.0 mg/mL of star copolymers and incubated for 4 h. For lysosome staining by LysoTracker, the cells were washed twice with PBS and then further incubated with LysoTracker Red (1.0 mM in PBS) for 20 min. The K$^+$-responsive star copolymer and LysoTracker were observed using a confocal laser scanning microscope LSM510 META NLO (Carl Zeiss Co. Ltd., Jena, Germany). A 488 nm argon laser was used for star copolymers, and a 543 nm HeNe laser was used for LysoTracker. The macrophage-selective targeting ability of polymer aggregates was further evaluated using flow cytometry. The number of polymer aggregates internalized into the three cell lines was compared using a fluorescence-activated cell sorter (FACS) Gallios (Beckman Coulter, Brea, CA). RAW264.7 cells, mouse fibroblast NIH/3T3 cells, and human hepatoma HepG2 cells were maintained in culture medium (RPMI for RAW264.7, DMEM for NIH/3T3 and

HepG2) with 10% fetal bovine serum and 1% penicillin−streptomycin at 37 °C and 5% CO$_2$. These cells were treated with a cell culture medium containing 1.0 mg/mL of the polymer nanoparticles for 4 h; the cells were washed twice with PBS. The fluorescent signal from the star copolymers internalized by each cell was quantified and analyzed using FlowJo software (BD Biosciences, Franklin Lakes, NJ).

■ RESULTS AND DISCUSSION

Synthesis and Characterization of HPG-g-NIPAM-co-BCAm-co-FMA. HPG-g-NIPAM-co-BCAm-co-FMA was synthesized following the synthetic route shown in Scheme 1. First, the terminal hydroxyl groups of HPG were converted into 2-bromoisobytyryl groups as initiators of the polymerization reaction. The successful introduction of initiator groups into the termini of HPG was confirmed via ^{1}H NMR spectra, which showed the proton signal around 1.98 ppm from −C−(CH$_3$)$_2$ protons (Figure 2). The conversion efficiency of the hydroxyl groups to Br initiator groups was evaluated by elemental analysis. The obtained conversion efficiency varied according to the amount of 2-bromoisobutyrylbromide added. The addition of 0.50, 0.75, and 1.00 equiv of 2-bromoisobutyrylbromide to hydroxyl groups of the HPG molecule resulted in conversion efficiencies of 36.8, 56.8, and 96.0% (corresponding to 15, 23, and 38 Br initiator groups per HPG), respectively. Hereafter, we refer to these macro-initiators with three different conversion efficiencies (15, 23, and 38 Br groups) as HPG-Br(1), HPG-Br(2), and HPG-Br(3), respectively. The successful synthesis of Me$_6$TREN as a ligand for ATRP polymerization was confirmed through ^{1}H NMR spectrum (Figure S1).

The star arms were polymerized by ATRP with the obtained macroinitiator. To determine the appropriate arm grafting density, macroinitiators with three different conversion efficiencies, HPG-Br(1), HPG-Br(2), and HPG-Br(3) were polymerized with only PNIPAM units (Scheme S1). The polymerization of NIPAM arms from PG was confirmed by ^{1}H NMR spectra, which showed the proton signals at around 1.03, 1.41 (and 1.93), 3.83, and 7.14 ppm, attributed to −C−CH$_3$,

$-CH-CH_2-$, $-C-CH-C-$, and $-C-NH-C=O$ protons, respectively, of polymerized NIPAM (Figure S2). The polymerization degree of each star arm was evaluated through the ^{1}H NMR measurement of the crude ATRP reaction solution (Figure S3). The grafted star copolymers, viz. HPG(1)-*g*-NIPAM, HPG(2)-*g*-NIPAM, and HPG(3)-*g*-NIPAM, obtained from HPG-Br(1), HPG-Br(2), and HPG-Br(3), respectively, showed polymerization degrees of 164, 184, and 165, respectively. The PNIPAM segment is known to show a temperature-dependent phase transition with a lower critical solution temperature (LCST) of 31 °C in water.[44] The obtained star copolymers also demonstrated thermo-responsive phase transitions with the same LCST of 34 °C regardless of the polymerization degree of the PNIPAM star arms (Figure S4). Notably, the HPG(3)-*g*-NIPAM solution was clouded even below the LCST, whereas the solutions of the other two polymers, viz. HPG(1)-*g*-NIPAM and HPG(2)-*g*-NIPAM, were transparent below the LCST. Additionally, as shown in Figure S5, HPG(1)-*g*-NIPAM and HPG(2)-*g*-NIPAM were aggregated, and their hydrodynamic diameters increased from 31.1 to 109 nm and from 32.6 to 87.7 nm in response to the temperature rising from 20 to 40 °C, whereas HPG(3)-*g*-NIPAM in water aggregated regardless of the temperature. It is suggested that the aggregation of HPG(3)-*g*-NIPAM was due to the higher graft density (0.12 nm^2/molecule) compared with those of HPG(1)-*g*-NIPAM (0.20 nm^2/molecule) and HPG(2)-*g*-NIPAM (0.31 nm^2/molecule) (Table S1), which prevents the temperature-responsive phase transition of NIPAM.[45,46] HPG(2)-*g*-NIPAM and PG(3)-*g*-NIPAM showed 23 and 40 grafted arms on the 1.2 nm PG, which was a higher grafting density than previously reported PNIPAM-based star polymers; for example, a star polymer consisting of 42 PNIPAM arms and a hyperbranched poly(glycidol) core with a size of 6.84 nm,[47] as well as one consisting of 52 PNIPAM arms and a hyperbranched polyester with a size of 3 nm were reported.[48] The high grafting density of the PNIPAM arms was reported to cause the collapse of the temperature-responsive phase transition because of the conformational alteration of the PNIPAM arms from mushroom to dense brush.[45,46] This explains why HPG(3)-*g*-NIPAM showed aggregation even below the LCST. Meanwhile, HPG(1)-*g*-NIPAM demonstrated a temperature-responsive phase transition owing to its appropriate arm density. Hence, HPG-Br(1) was selected as the macroinitiator to obtain the star copolymers.

Next, the BCAm unit was copolymerized with NIPAM from HPG via ATRP. The successful copolymerization of NIPAM and BCAm was confirmed by the FT-IR spectra (Figure 3), which showed the NIPAM peak from isopropyl groups at 1388 cm^{-1}, BCAm peaks from benzyl ethers at 1262 cm^{-1}, ether bonds at 1133 cm^{-1}, and amide bonds at 1650 and 1550 cm^{-1}. The successful copolymerization of NIPAM and BCAm was also confirmed from the ^{1}H NMR spectrum, which showed peaks from NIPAM units at 1.03, 1.41, 1.93, 3.83, and 7.14 ppm, and peaks from BCAm units at 3.4−4.1 ppm (Figure S2). From the ^{1}H NMR spectra of the reaction solution (Figure S6), the polymerization degree of NIPAM and BCAm units was calculated. The effect of the NIPAM-to-BCAm molar ratio in the ATRP solution on the copolymerization ratio of NIPAM and BCAm is shown in Figure 4. The ratio of the BCAm units in the obtained copolymer increased with increasing molar ratio in the reaction solution, showing an almost linear relationship. The ratio of the BCAm unit significantly affects
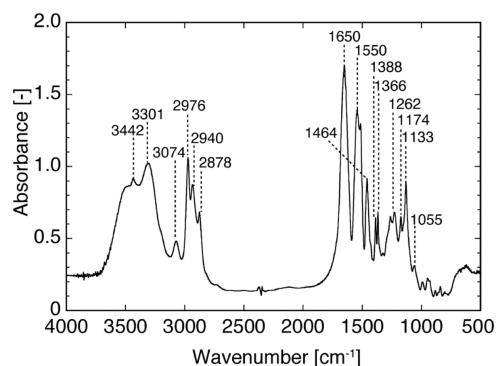
Figure 3. FT-IR spectra of HPG-*g*-NIPAM-*co*-BCAm-*co*-FMA. The presence of NIPAM was confirmed by the peaks from isopropyl groups at 1366 and 1388 cm^{-1} and those from CH$_3$ asymmetric deformation at 1133, 1174, and 1464 cm^{-1}. The presence of BCAm was also confirmed by the peaks from C−O stretching vibration in ethers at 1055 cm^{-1}, those from C−O asymmetric stretching vibration in benzyl ether at 1262 cm^{-1} in crown ethers at 1550 cm^{-1}, those from C−H asymmetric and symmetric stretching vibration at 2878, 2940, and 2976 cm^{-1}. The peaks from N−H stretching vibration at 3074, 3301, and 3442 cm^{-1} and C=O stretching vibration at 1650 cm^{-1} were from amide bonds. These peaks confirmed the successful ATRP reaction of NIPAM and BCAm.
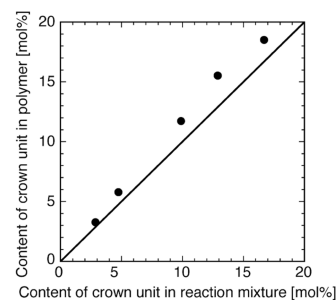

Figure 4. Dependence of copolymerization ratio of the crown unit in star arms on initial monomer feed in the reaction mixture.

the LCST of the obtained star copolymers. To render K$^+$-ion-responsiveness under physiological conditions, the LCST of the star copolymer needs to be below 37 °C without K$^+$ ions, whereas it needs to be higher than 37 °C in the presence of K$^+$ ions. In this study, we chose a star copolymer with a BCAm crown unit content of 15.5 mol %. The synthesized star copolymer showed the appropriate phase transition behavior in response to temperature and K$^+$ concentration.

Finally, NIPAM, BCAm, and FMA were copolymerized from the macroinitiator (the NIPAM/BCAm/FMA ratio was 100:15:1 in the initial reaction mixture) to obtain star copolymers with K$^+$ ion-responsive aggregation/dispersion and fluorescent on/off switching properties. The copolymerization of NIPAM and BCAm was confirmed from the ^{1}H NMR spectra of the resulting copolymer (Figure 2). The NIPAM copolymerization ratio of HPG-*g*-NIPAM-*co*-BCAm-*co*-FMA was 76.7, which is lower than that of HPG-*g*-NIPAM-*co*-BCAm (84.6).

Phase Transition Behavior and PL Switching of HPG-*g*-NIPAM-*co*-BCAm-*co*-FMA. The dependence of the phase transition behavior of the obtained HPG-*g*-NIPAM-*co*-BCAm-*co*-FMA star copolymer on temperature and K$^+$ ion concentration was evaluated by turbidity measurements. The LSCT decreased when hydrophobic groups were introduced

into the PNIPAM, whereas it increased with the introduction of hydrophilic groups. The LSCT of the star copolymer (35.6 °C) was higher than that of PNIPAM in water with 160 mM of NaCl because a small quantity of Na^+ ions was chelated in crown ethers of the BCAm unit. When the concentration of KCl was increased, the LSCT of the star copolymer increased, depending on the KCl concentration, reaching 47.2 °C with 160 mM KCl (Figure 5). The observed K^+-ion-responsive shift
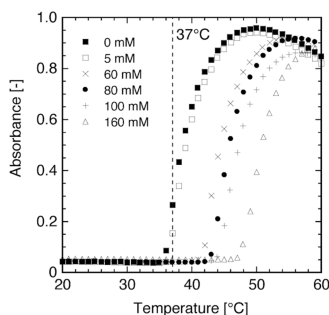
Figure 5. Temperature-dependent phase transition behaviors of the star copolymer in water with different K^+ concentration levels.

in the LCST can be explained by the selective host–guest complex formation of BCAm with K^+ ions, which subsequently alters the phase transition behavior of the neighboring NIPAM.

Changes in the colloidal size of the HPG-*g*-NIPAM-*co*-BCAm-*co*-FMA star copolymer in response to K^+ ions were evaluated by DLS (Figure 6). The star copolymer dispersed as
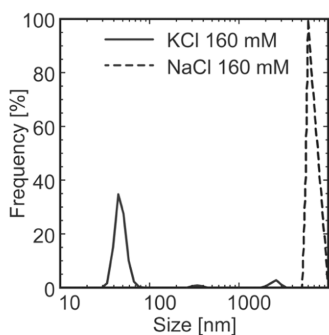
Figure 6. Hydrodynamic diameter of the star copolymer at the dispersion/aggregation states in water with 160 mM of KCl or 160 mM of NaCl was measured by DLS.

nanoparticles with a diameter of 80 nm in 160 mM KCl, whereas it aggregated into micron-sized particles in 160 mM NaCl at 37 °C. Even in the aggregated state, the star copolymers did not cause severe sedimentation; microparticles with a diameter of ~5.5 *μ*m were observed by microscopic observation in 160 mM NaCl (Figure S7).

Because we copolymerized FMA in star copolymer arms, it was expected that the shrinking of the copolymer arms and the resultant aggregation of polymer particles would cause the concentration quenching of FMA. In contrast, the swelling and dispersion of the star copolymers caused PL activation via dequenching. The phase transition-induced switching of PL due to quenching/dequenching was investigated by measuring the fluorescence intensity of the star copolymer solution in water during the temperature increase from 25 to 50 °C. The star copolymer solution showed a significant decrease in the PL signal between 32.5 and 35 °C (Figure 7a). This behavior is
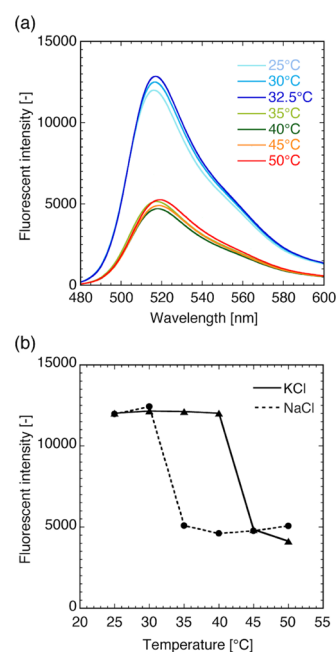

Figure 7. (a) PL spectra of star copolymers in water at different temperatures. (b) Peak PL intensity of star copolymer in water with different metal ions (160 mM KCl or 160 mM NaCl) at different temperatures.

consistent with the dispersion/aggregation transition observed in the turbidity test. PL switching from the ON to OFF state occurred between 30 and 35 °C with 160 mM NaCl, mimicking the environment of outside cells. In contrast, it occurred between 40 and 45 °C with 160 mM KCl, which mimics the intracellular environment (Figure 7b). Considering that the physiological temperature in the mammalian body is 37 °C, the star copolymer particles are expected to work as activatable PL probes responding to the intra/outer cellular environment.

Recently, K^+-responsive PL switching probes regulated by their higher hierarchical conformational change of materials have been intensively explored, such as pyrene excimer luminescent probes[26,49] and fluorophore-terminated G-quadruplex DNA-based probes.[50,51] Aggregation-induced emission (AIE)-based PL switching has also attracted attention.[52,53] We employed the K^+-responsive aggregation/dispersion transition of colloidal particles as a driving force for PL switching. We demonstrated K^+-responsive PL switching *via* the copolymerization of FMA with poly(NIPAM-*co*-BCAm) as star arms. This K^+-responsive aggregation/dispersion transition of star copolymers is expected to be utilized for other types of PL switches, such as an AIE-based PL switch, by altering FMA to other fluorescent molecules with AIE properties, e.g., tetraphenylethene.

Macrophage Targeting and PL Switching of HPG-*g*-NIPAM-*co*-BCAm-*co*-FMA. We further examined the possibility of macrophage-selective labeling of HPG-*g*-NIPAM-*co*-BCAm-*co*-FMA star copolymers using K^+-ion-responsive dispersion/aggregation transition and PL switching. The cultured mouse macrophage RAW264.7 cells were incubated with the star copolymers at 37 °C under 5% CO_2 for 4 h, followed by confocal laser microscopic observation. The star copolymers at the aggregation state did not show high fluorescence in the cell culture medium outside the macro-
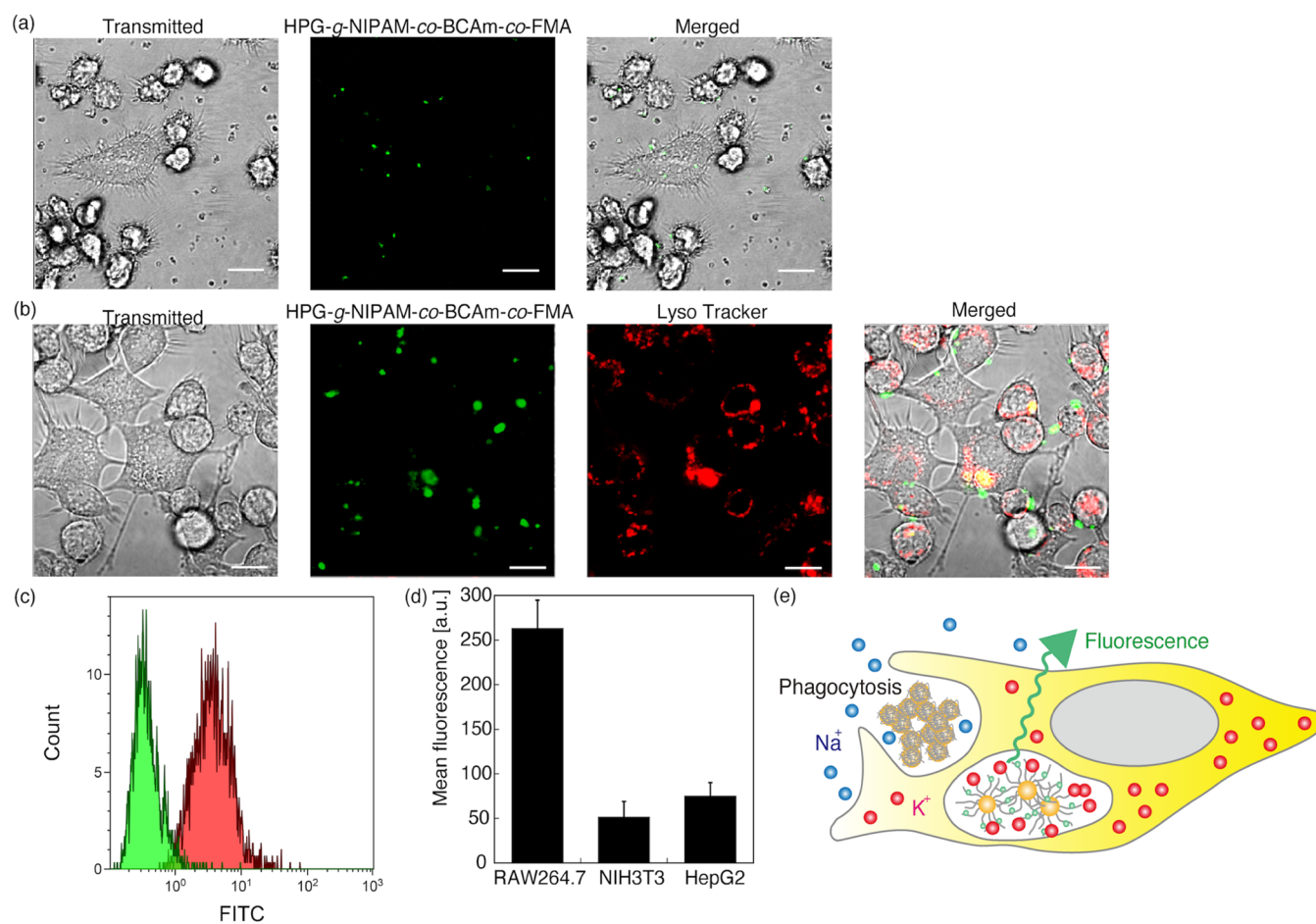
Figure 8. Macrophage targeting and PL switching in macrophages of the star copolymers. (a) Confocal microscopic images of the star copolymer inside/outside macrophages, and (b) colocalization of the star copolymer inside macrophages with LysoTracker. Scale bars indicate 10 μm. (c) PL intensity from the star copolymers internalized into each macrophage cell was evaluated via FACS. The green histogram indicates control cells without the star copolymer application, and the red histogram indicates cells incubated with the star copolymers. (d) PL intensity from the star copolymer internalized into different types of cells, macrophages, fibroblast cells, and cancer cells measured by FACS. (e) Schematic of macrophage targeting and PL switching of the star copolymer responding to K^+ inside macrophages.

phages with 4 mM K^+. In contrast, they showed significant PL following cellular uptake by RAW264.7 (Figure 8a). Considering the micron-sized hydrodynamic diameter of the star copolymer particles in the aggregated state, they were internalized into macrophages via phagocytosis. The PL signals of star copolymers in macrophages colocalized with LysoTracker (Figure 8b), indicating their localization in phagosomes. These results suggest that the PL switching of star copolymers occurred due to the transition from the aggregated microparticle state to the dispersed nanoparticle state and subsequent fluorescent dequenching in response to a high concentration of K^+ inside phagosomes.

The micron size of HPG-*g*-NIPAM-*co*-BCAm-*co*-FMA in the outer cellular environment is also expected to prevent its uptake by other types of cells. To examine this possibility, we incubated the star copolymers with mouse macrophage RAW264.7, mouse fibroblast NIH/3T3, and human hepatoblastoma HepG2 cells. This was followed by comparing their cellular uptake amounts using FACS. Macrophages treated with the star copolymer exhibited a significantly higher PL signal than control cells without incubation with star copolymers (Figure 8c), suggesting the internalization of star copolymers into cells. The PL signal of star copolymers internalized into RAW264.7 cells was more than 5 times higher

than that of NIH/3T3 cells and HepG2 cells (Figure 8d). This could be because the micron-sized star copolymers in the aggregated state could be taken up only through phagocytosis. These results suggest using HPG-*g*-NIPAM-*co*-BCAm-*co*-FMA star copolymers as macrophage-targeted fluorescent imaging agents (Figure 8e).

Since macrophages are key players in inflammation, our results suggest the potential of HPG-*g*-NIPAM-*co*-BCAm-*co*-FMA as a probe for the diagnosis of inflammation-related diseases. In addition, because K^+ ions are related to a wide range of physiological phenomena, the developed K^+-responsive aggregation/dispersion system is expected to be applied in various biomedical fields, which will be investigated in future studies.

■ CONCLUSIONS

We developed a K^+-responsive dispersion/aggregation transition colloidal star copolymer system based on hydrophilic and biocompatible HPG, grafted with the thermo-responsive PNIPAM unit and ion-selective recognition unit BCAm. The grafting density of the copolymers to a macroinitiator and the copolymerization ratio of PNIPAM to BCAm were successfully controlled and optimized. The precisely designed star copolymer particle demonstrated a dispersion/aggregation

phase transition in response to temperature and the presence of K$^+$ at a physiological temperature (37 °C). The copolymerization of K$^+$-responsive BCAm units with PNIPAM has been demonstrated in numerous studies to accomplish dual responsiveness to metal ions and temperature. The poly(NIPAM-*co*-BCAm)-grafted microcapsules were investigated as a K$^+$-responsive reactor of enzymes that controlled the permeability of substrates through ion-selective gates,[35] while poly(NIPAM-*co*-BCAm) microspheres demonstrated a swell–shrink phase transition depending on the temperature and formed reversible aggregates responding to K$^+$ in the shrink state.[36] However, since the hydrophobicity of poly(NIPAM-*co*-BCAm) drastically changes above the LCST, the formation of precipitation in the aggregated state in the presence of K$^+$ has restricted its potential as a K$^+$-responsive colloidal material. One of the advantages of star polymers is their structural design flexibility via the combination of a core and arms, which enables various functional tunings. In this study, by combining the K$^+$-responsive poly(NIPAM-*co*-BCAm) arms with a hydrophilic HPG core for the first time, we prevented the precipitation of star copolymers above the LCST. As a result, the supramolecular host–guest interaction between the metal ion and crown ether was converted into a macroscopic transition between the aggregation and dispersion of the star copolymers, similar to immunoprecipitation. FMA was further copolymerized with NIPAM and BCAm to exhibit K$^+$-responsive PL switching of the star copolymers triggered by their aggregation/dispersion. Moreover, macrophage-selective targeting and visualization were performed as an example of their application. The developed HPG-*g*-NIPAM-*co*-BCAm-*co*-FMA star copolymer is expected to apply to various biomedical fields involving K$^+$ ions.

■ ASSOCIATED CONTENT

Ⓢ Supporting Information

The Supporting Information is available free of charge at https://pubs.acs.org/doi/10.1021/acsomega.2c06763.

> ^{1}H NMR spectrum of Tris(2-dimethyl aminoethyl)-amine in CDCl$_3$ (Figure S1); synthetic route to HPG-*g*-NIPAM (Scheme S1); ^{1}H NMR spectra of HPG-*g*-NIPAM and HPG-*g*-NIPAM-*co*-BCAm in DMSO-*d$_6$* (Figure S2); ^{1}H NMR spectra of ATRP reaction solution of HPG-*g*-NIPAM in DMSO-*d$_6$* (Figure S3); temperature-dependent phase transition behavior of HPG-*g*-NIPAM with different grafting ratios (Figure S4); hydrodynamic diameters of HPG-*g*-NIPAM with different grafting ratios in water at different temperatures (20 and 40 °C), as measured by DLS (Figure S5); characterization of HPG-*g*-NIPAM synthesized from HPG-Br with different amounts of initiator groups (Table S1); ^{1}H NMR spectra of the ATRP reaction solution of HPG-*g*-NIPAM-*co*-BCAm in DMSO-*d$_6$* (Figure S6); and confocal microscopy image of the star copolymer in aggregated state in water with 160 mM NaCl (Figure S7) (PDF)

■ AUTHOR INFORMATION

Corresponding Author

Taichi Ito − *Department of Bioengineering and Department of Chemical System Engineering, The University of Tokyo, Tokyo 113-8656, Japan; Center for Disease Biology and Integrative Medicine, The University of Tokyo, Tokyo 113-0033, Japan;* ⓘ orcid.org/0000-0002-1589-8242; Phone: +81-3-5841-1425; Email: taichi@m.u-tokyo.ac.jp

Authors

Noriko Nakamura − *Institute of Engineering Innovation, The University of Tokyo, Tokyo 113-8656, Japan*

Seiichi Ohta − *Institute of Engineering Innovation, The University of Tokyo, Tokyo 113-8656, Japan; Department of Bioengineering and Department of Chemical System Engineering, The University of Tokyo, Tokyo 113-8656, Japan*

Mariko Yamada − *Department of Bioengineering, The University of Tokyo, Tokyo 113-8656, Japan*

Yukimitsu Suzuki − *Department of Chemical System Engineering, The University of Tokyo, Tokyo 113-8656, Japan*

Natsuko F. Inagaki − *Center for Disease Biology and Integrative Medicine, The University of Tokyo, Tokyo 113-0033, Japan*

Takeo Yamaguchi − *Institute of Innovative Research, Tokyo Institute of Technology, Yokohama 226-8503, Japan;* ⓘ orcid.org/0000-0001-9043-4408

Complete contact information is available at:
https://pubs.acs.org/10.1021/acsomega.2c06763

Notes

The authors declare no competing financial interest.

■ REFERENCES

(1) Stuart, M. A. C.; Huck, W. T. S.; Genzer, J.; Müller, M.; Ober, C.; Stamm, M.; Sukhorukov, G. B.; Szleifer, I.; Tsukruk, V. V.; Urban, M.; et al. Emerging applications of stimuli-responsive polymer materials. *Nat. Mater.* **2010**, *9*, 101−113.

(2) Ionov, L.; Minko, S.; Stamm, M.; Gohy, J.-F.; Jérôme, R.; Scholl, A. Reversible Chemical Patterning on Stimuli-Responsive Polymer Film: Environment-Responsive Lithography. *J. Am. Chem. Soc.* **2003**, *125*, 8302−8306.

(3) Tokarev, I.; Minko, S. Stimuli-responsive hydrogel thin films. *Soft Matter* **2009**, *5*, 511−524.

(4) Granville, A. M.; Boyes, S. G.; Akgun, B.; Foster, M. D.; Brittain, W. J. Thermoresponsive Behavior of Semifluorinated Polymer Brushes. *Macromolecules* **2005**, *38*, 3263−3270.

(5) Li, D.; Xu, L.; Wang, J.; Gautrot, J. E. Responsive Polymer Brush Design and Emerging Applications for Nanotheranostics. *Adv. Healthcare Mater.* **2021**, *10*, No. 2000953.

(6) Kim, J.; Yoon, J.; Hayward, R. C. Dynamic display of biomolecular patterns through an elastic creasing instability of stimuli-responsive hydrogels. *Nat. Mater.* **2010**, *9*, 159−164.

(7) Yoon, J.; Bian, P.; Kim, J.; McCarthy, T. J.; Hayward, R. C. Local Switching of Chemical Patterns through Light-Triggered Unfolding of Creased Hydrogel Surfaces. *Angew. Chem., Int. Ed.* **2012**, *51*, 7146−7149.

(8) Motornov, M.; Roiter, Y.; Tokarev, I.; Minko, S. Stimuli-responsive nanoparticles, nanogels and capsules for integrated multifunctional intelligent systems. *Prog. Polym. Sci.* **2010**, *35*, 174−211.

(9) Kuckling, D.; Wycisk, A. Stimuli-responsive star polymers. *J. Polym. Sci., Part A: Polym. Chem.* **2013**, *51*, 2980−2994.

(10) Ren, J. M.; McKenzie, T. G.; Fu, Q.; Wong, E. H. H.; Xu, J.; An, Z.; Shanmugam, S.; Davis, T. P.; Boyer, C.; Qiao, G. G. Star Polymers. *Chem. Rev.* **2016**, *116*, 6743−6836.

(11) Dozier, W. D.; Huang, J. S.; Fetters, L. J. Colloidal nature of star polymer dilute and semidilute solutions. *Macromolecules* **1991**, *24*, 2810−2814.

(12) Likos, C. N.; Löwen, H.; Watzlawek, M.; Abbas, B.; Jucknischke, O.; Allgaier, J.; Richter, D. Star Polymers Viewed as Ultrasoft Colloidal Particles. *Phys. Rev. Lett.* **1998**, *80*, 4450−4453.

(13) Vlassopoulos, D. Colloidal star polymers: Models for studying dynamically arrested states in soft matter. *J. Polym. Sci., Part B: Polym. Phys.* **2004**, *42*, 2931−2941.

(14) Navath, R. S.; Wang, B.; Kannan, S.; Romero, R.; Kannan, R. M. Stimuli-responsive star poly(ethylene glycol) drug conjugates for improved intracellular delivery of the drug in neuroinflammation. *J. Controlled Release* **2010**, *142*, 447−456.

(15) Liu, J.; Pang, Y.; Huang, W.; Zhu, Z.; Zhu, X.; Zhou, Y.; Yan, D. Redox-Responsive Polyphosphate Nanosized Assemblies: A Smart Drug Delivery Platform for Cancer Therapy. *Biomacromolecules* **2011**, *12*, 2407−2415.

(16) Nakagawa, Y.; Amano, Y.; Nakasako, S.; Ohta, S.; Ito, T. Biocompatible Star Block Copolymer Hydrogel Cross-linked with Calcium Ions. *ACS Biomater. Sci. Eng.* **2015**, *1*, 914−918.

(17) Nakagawa, Y.; Ohta, S.; Sugahara, A.; Okubo, M.; Yamada, A.; Ito, T. In Vivo Redox-Responsive Sol−Gel/Gel−Sol Transition of Star Block Copolymer Solution Based on Ionic Cross-Linking. *Macromolecules* **2017**, *50*, 5539−5548.

(18) Nakagawa, Y.; Ohta, S.; Nakamura, M.; Ito, T. 3D inkjet printing of star block copolymer hydrogels cross-linked using various metallic ions. *RSC Adv.* **2017**, *7*, 55571−55576.

(19) Lin, H.-H.; Cheng, Y.-L. In-Situ Thermoreversible Gelation of Block and Star Copolymers of Poly(ethylene glycol) and Poly(N-isopropylacrylamide) of Varying Architectures. *Macromolecules* **2001**, *34*, 3710−3715.

(20) Bao, Y.; De Keersmaecker, H.; Corneillie, S.; Yu, F.; Mizuno, H.; Zhang, G.; Hofkens, J.; Mendrek, B.; Kowalczuk, A.; Smet, M. Tunable Ratiometric Fluorescence Sensing of Intracellular pH by Aggregation-Induced Emission-Active Hyperbranched Polymer Nanoparticles. *Chem. Mater.* **2015**, *27*, 3450−3455.

(21) Huang, Y.; Qiu, F.; Chen, D.; Shen, L.; Xu, S.; Guo, D.; Su, Y.; Yan, D.; Zhu, X. Color-Convertible, Unimolecular, Micelle-Based, Activatable Fluorescent Probe for Tumor-Specific Detection and Imaging In Vitro and In Vivo. *Small* **2017**, *13*, No. 1604062.

(22) Lambeth, R. H.; Ramakrishnan, S.; Mueller, R.; Poziemski, J. P.; Miguel, G. S.; Markoski, L. J.; Zukoski, C. F.; Moore, J. S. Synthesis and Aggregation Behavior of Thermally Responsive Star Polymers. *Langmuir* **2006**, *22*, 6352−6360.

(23) Reeves, E. P.; Lu, H.; Jacobs, H. L.; Messina, C. G.; Bolsover, S.; Gabella, G.; Potma, E. O.; Warley, A.; Roes, J.; Segal, A. W. Killing activity of neutrophils is mediated through activation of proteases by K+ flux. *Nature* **2002**, *416*, 291−297.

(24) Yamauchi, A.; Hayashita, T.; Nishizawa, S.; Watanabe, M.; Teramae, N. Benzo-15-crown-5 Fluoroionophore/γ-Cyclodextrin Complex with Remarkably High Potassium Ion Sensitivity and Selectivity in Water. *J. Am. Chem. Soc.* **1999**, *121*, 2319−2320.

(25) Xia, W.-S.; Schmehl, R. H.; Li, C.-J. A Highly Selective Fluorescent Chemosensor for K+ from a Bis-15-Crown-5 Derivative. *J. Am. Chem. Soc.* **1999**, *121*, 5599−5600.

(26) Yamauchi, A.; Hayashita, T.; Kato, A.; Nishizawa, S.; Watanabe, M.; Teramae, N. Selective Potassium Ion Recognition by Benzo-15-crown-5 Fluoroionophore/γ-Cyclodextrin Complex Sensors in Water. *Anal. Chem.* **2000**, *72*, 5841−5846.

(27) Kim, J.; McQuade, D. T.; McHugh, S. K.; Swager, T. M. Ion-Specific Aggregation in Conjugated Polymers: Highly Sensitive and Selective Fluorescent Ion Chemosensors. *Angew. Chem., Int. Ed.* **2000**, *39*, 3868−3872.

(28) Irie, M.; Misumi, Y.; Tanaka, T. Stimuli-responsive polymers: chemical induced reversible phase separation of an aqueous solution of poly(N-isopropylacrylamide) with pendent crown ether groups. *Polymer* **1993**, *34*, 4531−4535.

(29) Mi, P.; Ju, X.-J.; Xie, R.; Wu, H.-G.; Ma, J.; Chu, L.-Y. A novel stimuli-responsive hydrogel for K+-induced controlled-release. *Polymer* **2010**, *51*, 1648−1653.

(30) Wu, H.-G.; Ju, X.-J.; Xie, R.; Liu, Y.-M.; Deng, J.-G.; Niu, C. H.; Chu, L.-Y. A novel ion-imprinted hydrogel for recognition of potassium ions with rapid response. *Polym. Adv. Technol.* **2011**, *22*, 1389−1394.

(31) Liu, Z.; Luo, F.; Ju, X.-J.; Xie, R.; Luo, T.; Sun, Y.-M.; Chu, L.-Y. Positively K+-Responsive Membranes with Functional Gates Driven by Host−Guest Molecular Recognition. *Adv. Funct. Mater.* **2012**, *22*, 4742−4750.

(32) Ito, T.; Hioki, T.; Yamaguchi, T.; Shinbo, T.; Nakao, S.-i.; Kimura, S. Development of a Molecular Recognition Ion Gating Membrane and Estimation of Its Pore Size Control. *J. Am. Chem. Soc.* **2002**, *124*, 7840−7846.

(33) Ito, T.; Yamaguchi, T. Osmotic Pressure Control in Response to a Specific Ion Signal at Physiological Temperature Using a Molecular Recognition Ion Gating Membrane. *J. Am. Chem. Soc.* **2004**, *126*, 6202−6203.

(34) Ito, T.; Yamaguchi, T. Nonlinear Self-Excited Oscillation of a Synthetic Ion-Channel-Inspired Membrane. *Angew. Chem., Int. Ed.* **2006**, *45*, 5630−5633.

(35) Akamatsu, K.; Ito, T.; Yamaguchi, T. Development of Enzyme-Encapsulated Microcapsule Reactors with Ion-Responsive Shell Membranes. *J. Chem. Eng. Jpn.* **2007**, *40*, 590−597.

(36) Ju, X.-J.; Liu, L.; Xie, R.; Niu, C. H.; Chu, L.-Y. Dual thermo-responsive and ion-recognizable monodisperse microspheres. *Polymer* **2009**, *50*, 922−929.

(37) Seiler, M. Hyperbranched polymers: Phase behavior and new applications in the field of chemical engineering. *Fluid Phase Equilib.* **2006**, *241*, 155−174.

(38) Voit, B. I.; Lederer, A. Hyperbranched and Highly Branched Polymer Architectures-Synthetic Strategies and Major Characterization Aspects. *Chem. Rev.* **2009**, *109*, 5924−5973.

(39) Wilms, D.; Stiriba, S.-E.; Frey, H. Hyperbranched Polyglycerols: From the Controlled Synthesis of Biocompatible Polyether Polyols to Multipurpose Applications. *Acc. Chem. Res.* **2010**, *43*, 129−141.

(40) Abbina, S.; Vappala, S.; Kumar, P.; Siren, E. M. J.; La, C. C.; Abbasi, U.; Brooks, D. E.; Kizhakkedathu, J. N. Hyperbranched polyglycerols: recent advances in synthesis, biocompatibility and biomedical applications. *J. Mater. Chem. B* **2017**, *5*, 9249−9277.

(41) Lee, C. C.; MacKay, J. A.; Fréchet, J. M. J.; Szoka, F. C. Designing dendrimers for biological applications. *Nat. Biotechnol.* **2005**, *23*, 1517−1526.

(42) Shin, K.; Suh, H.-W.; Grundler, J.; Lynn, A. Y.; Pothupitiya, J. U.; Moscato, Z. M.; Reschke, M.; Bracaglia, L. G.; Piotrowski-Daspit, A. S.; Saltzman, W. M. Polyglycerol and Poly(ethylene glycol) exhibit different effects on pharmacokinetics and antibody generation when grafted to nanoparticle surfaces. *Biomaterials* **2022**, *287*, No. 121676.

(43) Queffelec, J.; Gaynor, S. G.; Matyjaszewski, K. Optimization of Atom Transfer Radical Polymerization Using Cu(I)/Tris(2-(dimethylamino)ethyl)amine as a Catalyst. *Macromolecules* **2000**, *33*, 8629−8639.

(44) Heskins, M.; Guillet, J. E. Solution Properties of Poly(N-isopropylacrylamide). *J. Macromol. Sci., Part A: Chem.* **1968**, *2*, 1441−1455.

(45) Balamurugan, S.; Mendez, S.; Balamurugan, S. S.; O'Brien, M. J.; López, G. P. Thermal Response of Poly(N-isopropylacrylamide) Brushes Probed by Surface Plasmon Resonance. *Langmuir* **2003**, *19*, 2545−2549.

(46) Ishida, N.; Biggs, S. Effect of Grafting Density on Phase Transition Behavior for Poly(N-isopropylacryamide) Brushes in Aqueous Solutions Studied by AFM and QCM-D. *Macromolecules* **2010**, *43*, 7269−7276.

(47) Luo, S.; Hu, X.; Zhang, Y.; Ling, C.; Liu, X.; Chen, S. Synthesis of thermoresponsive unimolecular polymeric micelles with a hydrophilic hyperbranched poly(glycidol) core. *Polym. J.* **2011**, *43*, 41−50.

(48) Luo, S.; Xu, J.; Zhu, Z.; Wu, C.; Liu, S. Phase Transition Behavior of Unimolecular Micelles with Thermoresponsive Poly(N-isopropylacrylamide) Coronas. *J. Phys. Chem. B* **2006**, *110*, 9132−9139.

(49) Nagatoishi, S.; Nojima, T.; Juskowiak, B.; Takenaka, S. A pyrene-labeled G-quadruplex oligonucleotide as a fluorescent probe for potassium ion detection in biological applications. *Angew. Chem., Int. Ed.* **2005**, *44*, 5067−5070.

(50) He, F.; Tang, Y.; Wang, S.; Li, Y.; Zhu, D. Fluorescent amplifying recognition for DNA G-quadruplex folding with a cationic conjugated polymer: a platform for homogeneous potassium detection. *J. Am. Chem. Soc.* **2005**, *127*, 12343−12346.

(51) Ueyama, H.; Takagi, M.; Takenaka, S. A novel potassium sensing in aqueous media with a synthetic oligonucleotide derivative. Fluorescence resonance energy transfer associated with Guanine quartet-potassium ion complex formation. *J. Am. Chem. Soc.* **2002**, *124*, 14286−14287.

(52) Lu, D.; He, L.; Wang, Y.; Xiong, M.; Hu, M.; Liang, H.; Huan, S.; Zhang, X.-B.; Tan, W. Tetraphenylethene derivative modified DNA oligonucleotide for in situ potassium ion detection and imaging in living cells. *Talanta* **2017**, *167*, 550−556.

(53) Wang, X.; Hu, J.; Liu, T.; Zhang, G.; Liu, S. Highly sensitive and selective fluorometric off−on K$^+$ probe constructed via host−guest molecular recognition and aggregation-induced emission. *J. Mater. Chem.* **2012**, *22*, 8622−8628.